Cell, Vol. 95, 259–268, October 16, 1998, Copyright ©1998 by Cell Press

Crystal Structure of the Dbl and Pleckstrin Homology Domains from the Human Son of Sevenless Protein

Stephen M. Soisson,* Anjaruwee S. Nimnual,† Marc Uy,* Dafna Bar-Sagi,† and John Kuriyan*‡
*Howard Hughes Medical Institute
The Rockefeller University
New York, New York 10021
†Department of Molecular Genetics and Microbiology
State University of New York at Stony Brook
Stony Brook, New York 11794

Summary

Proteins containing Dbl homology (DH) domains activate Rho-family GTPases by functioning as specific guanine nucleotide exchange factors. All known DH domains have associated C-terminal pleckstrin homology (PH) domains that are implicated in targeting and regulatory functions. The crystal structure of a fragment of the human Son of sevenless protein containing the DH and PH domains has been determined at 2.3 Å resolution. The entirely α-helical DH domain is unrelated in architecture to other nucleotide exchange factors. The active site of the DH domain, identified on the basis of sequence conservation and structural features, lies near the interface between the DH and PH domains. The structure suggests that ligation of the PH domain will be coupled structurally to the GTPase binding site.

Introduction

Members of the Ras superfamily of small GTPases act as molecular switches by cycling between an active, GTP-bound state and an inactive, GDP-bound state. The ~60 members of the Ras GTPase superfamily, which play a central role in the regulation of both normal and transformed cell growth, can be divided into six subgroups on the basis of primary sequence similarities (reviewed by Bourne et al., 1991; Boguski and McCormick, 1993). One subgroup, the Rho family GTPases, is important for the regulation of actin-based cytoskeletal reorganizations. Signaling through Rho GTPases is necessary for the determination of cell polarity, cell adhesion and motility, morphogenesis, and contractile responses such as those required for cytokinesis (reviewed by Hall, 1998). Rho GTPases are essential downstream components of the Ras transformation pathway (Qiu et al., 1995), and they control transcriptional events that are required for cell growth, differentiation, and apoptosis (Coso et al., 1995; Hill et al., 1995; Minden et al., 1995; Olson et al., 1995).

Guanine nucleotide exchange factors activate GTPases by stimulating the exchange of GDP for GTP, thereby initiating signaling. For the Rho family of GTPases, this is accomplished by proteins containing Dbl homology domains (reviewed by Cerione and Zheng, 1996; Whitehead et al., 1997). Dbl homology (DH) domains were identified initially as a ~250-residue region of sequence similarity between the transforming gene of diffuse B cell lymphoma (Dbl) and the Cdc24 protein from *S. cerevisiae* (Eva and Aaronson, 1985; Ron et al., 1991). Both Dbl and Cdc24 were later demonstrated to be selective nucleotide exchange factors for the Rho-family GTPase, Cdc42 (Hart et al., 1991; Zheng et al., 1994). Subsequent studies aimed at identifying new oncogenes have uncovered over 20 proteins containing DH domains, making the Dbl family one of the largest groups of oncoproteins currently known (Figure 1) (reviewed by Cerione and Zheng, 1996; Whitehead et al., 1997). Dominant negative alleles of Rho GTPases inhibit transformation by Dbl-family proteins, which further supports the hypothesis that these proteins exert their effects by activating the Rho signaling pathways (Zheng et al., 1995; Whitehead et al., 1996). Most DH domain–containing proteins are probably specialized components of particular signal transduction pathways, since they have been demonstrated to possess guanine nucleotide exchange factor activity for distinct subsets of the Rho-family GTPases (Whitehead et al., 1997). Several DH domain–containing proteins have been directly linked to disease manifestation. For example, the Tiam-1 protein was demonstrated to promote tumor invasion and metastasis in mice, suggesting a direct link between Rho-family induced cytoskeletal rearrangements and the progression of cancer (Habets et al., 1994).

Interestingly, all DH domains identified thus far are followed immediately at their C terminus by a pleckstrin homology (PH) domain (Whitehead et al., 1997). PH domains are ~100-residue modules that are found in a large number of proteins involved in intracellular signaling and cytoskeletal reorganizations (reviewed by Lemmon and Ferguson, 1998). It is now generally accepted that PH domains serve to target their host proteins to the plasma membrane primarily through interactions with specific phospholipids (Lemmon and Ferguson, 1998); however, some PH domains may also interact with other proteins such as protein kinase C and the βγ subunits of heterotrimeric G proteins (Yao et al., 1994; Konishi et al., 1995; Pitcher et al., 1995). The invariant juxtaposition of DH and PH domains suggests that structural relationships between the two modules may be critical for functionality.

The ubiquitously expressed Son of sevenless (Sos) protein was first identified genetically as a component of the *sevenless* signaling pathway that controls *Drosophila* compound eye development (reviewed by Raabe, 1998). Sos contains two distinct guanine nucleotide exchange factor domains that are specific for the closely related Ras and Rho family GTPases, respectively (Figure 2). Sos serves as the primary link between receptor tyrosine kinase signaling and the Ras signaling pathways through its Ras exchange factor domain, which is homologous to the catalytic domain of Cdc25 (Bar-Sagi, 1994). Sos also contains a Dbl homology domain that has recently been shown to activate Rac1 by acting as

‡To whom correspondence should be addressed (e-mail: kuriyan@rockvax.rockefeller.edu).

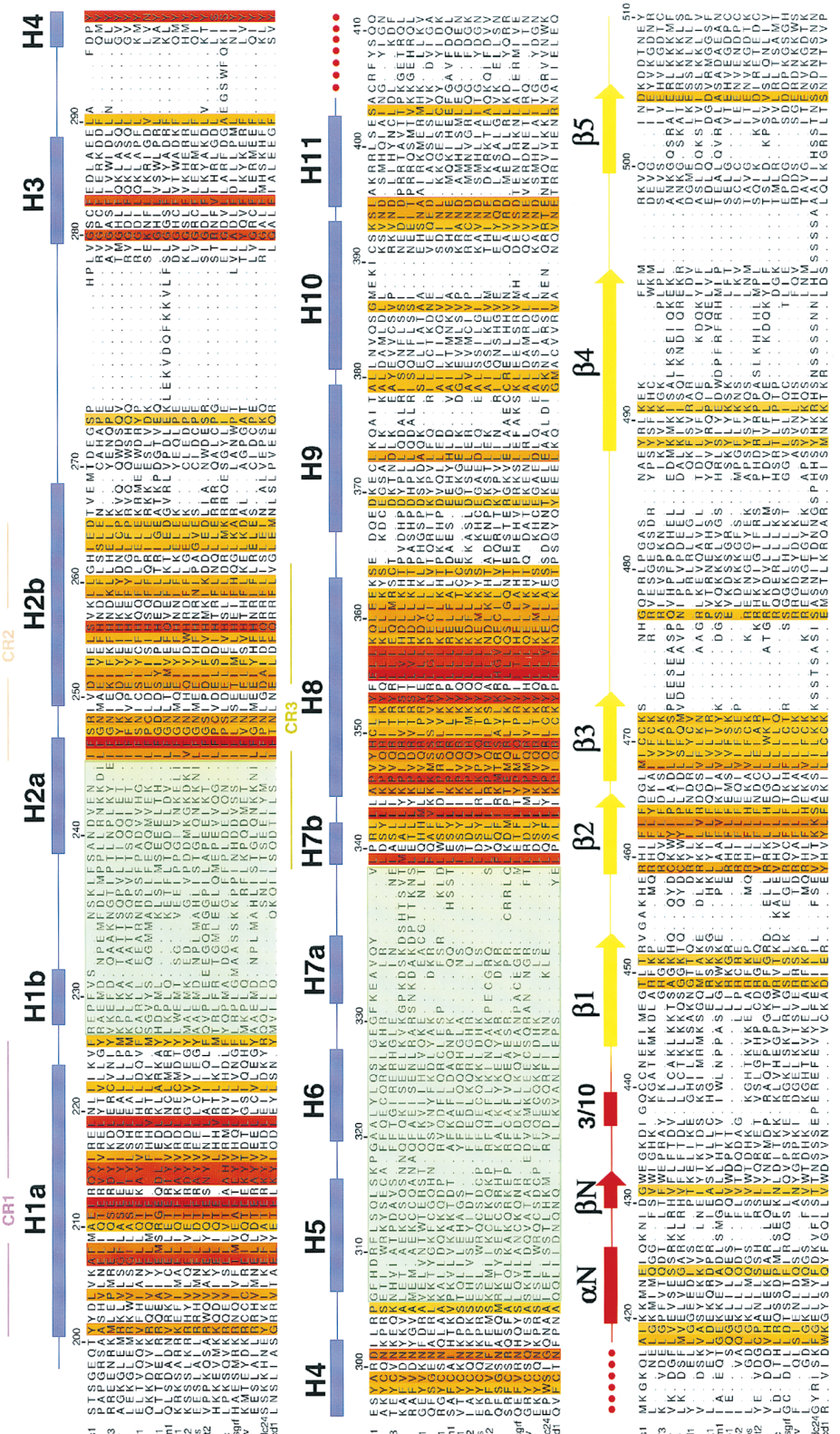

Figure 1. Sequence Alignment of DH-PH Domains

Sequences were chosen and aligned as described in Experimental Procedures. Numbering is relative to Sos. Overall sequence identity (0%–100%) at each position is shaded as a color gradient from white to yellow to red. For clarity, only positions with identities above 40% are shaded in this figure. Regions where there is very little sequence similarity are shaded green to indicate that the alignment is unreliable

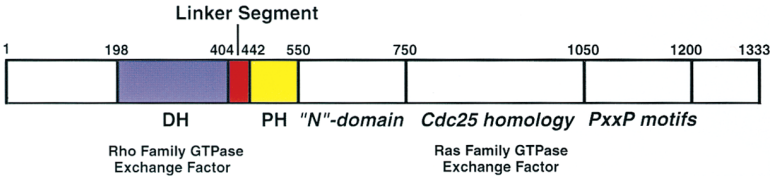

Figure 2. Domain Structure of the Sos Protein

The construct used for structure determination is depicted in color. The DH domain is colored blue, the PH domain is yellow, and the linker segment discussed in the text is colored red. The N domain, as described previously, is a structural component of the Ras exchange factor region (Boriack-Sjodin et al., 1998). PxxP motifs are SH3-domain binding sites (Bar-Sagi, 1994).

a nucleotide exchange factor, thereby providing a link between the Ras-family and Rho-family GTPase signaling pathways (Nimnual et al., 1998). Phospholipid binding to the DH-associated PH domain has been implicated in the stimulation of exchange factor activity of both Sos and Vav, another Dbl-related protein (Han et al., 1998; Ma et al., 1998; Nimnual et al., 1998).

Despite high sequence similarity and a conserved three-dimensional structure, each subgroup of the Ras family GTPases has its own distinct set of highly specific exchange factors. Somewhat surprisingly, recent determinations of the structures of some of these guanine nucleotide exchange factors have revealed that they are structurally unrelated. For example, the Ras exchange factor region of human Sos1 (Boriack-Sjodin et al., 1998), the Arf exchange factor Sec7-related domain from ARNO (Mossessova et al., 1998; Cherfils et al., 1998), the Ran exchange factor, RCC1 (Renault et al., 1998), and the Rab exchange factor, Mss4 (Yu and Schreiber, 1995) display no structural similarities. Currently, EF-Tu/EF-Ts (Kawashima et al., 1996; Wang et al., 1997) and Ras/Sos (Boriack-Sjodin et al., 1998) are the only examples of guanine nucleotide exchange factors whose structures have been determined in complex with their cognate GTPases. Of these, Ras/Sos is the only structure of a Ras superfamily GTPase in complex with its exchange factor. In contrast to the Ras exchange factor domain, for which a considerable body of mechanistic information is now available (see for example, Lenzen et al., 1998), a detailed enzymological and structural characterization of a Dbl homology domain has yet to be performed.

Here, we present the structure of the tandem DH and PH domains of human Sos1 (which we shall refer to as Sos). The architecture of the DH domain is unrelated to that of other nucleotide exchange factors. The PH domain is attached to one end of the elongated, all-helical, DH domain, resulting in an overall L-shaped DH-PH unit. Sequence similarity within DH and PH domains suggests that the folds of both domains are generally conserved in all DH-PH domain–containing proteins. The interface between the DH and PH modules is, however, highly variable in sequence, indicating that the relative disposition of these domains may be altered in other proteins. Analysis of sequence similarities reveals a contiguous patch of highly conserved surface residues presented by two α helices in the DH domain. Mutations affecting exchange factor activity (Hart et al., 1994; Alberts and Treisman, 1998; Steven et al., 1998) localize almost exclusively to this region, indicating that it is involved in GTPase binding and exchange factor activity. The GTPase binding site is located in the elbow of the DH-PH unit in such a manner that a structural connection is established between the catalytic site of the exchange factor and the phospholipid binding site of the PH domain.

Results and Discussion

Structure Determination

A fragment of human Sos1 that includes the entire DH and PH domains (residues 180–551) was expressed in *Escherichia coli* and purified to homogeneity. A stable and slightly smaller subfragment (residues 189–551) was identified by proteolysis with elastase. The elastase-resistant fragment was subcloned, expressed in *E. coli*, and purified for use in crystallization experiments. Crystals form in the monoclinic space group C2, with one molecule in the asymmetric unit, and diffract X-rays to better than 2.3 Å resolution using synchrotron radiation. The structure was determined using multiwavelength anomalous dispersion (MAD) from crystals of selenomethionyl-subsituted protein (Table 1). The solvent-flattened experimental MAD map calculated at 2.3 Å resolution was of exceptional quality and allowed a nearly complete model of the DH and PH domains to be built. The final refined DH-PH model has a free R value of 26.8% and a conventional crystallographic R value of 22.6% using all data from 30–2.3 Å (26.6% and 22.5%, respectively, for reflections with $|F| > 2\sigma|F|$) and consists of residues 198–550 of Sos and 69 water molecules. The N-terminal residues 189–197, as well as residues 405–417, which are part of the connector between the DH and PH domains, are disordered and are not included in the final model.

Structural Overview

The DH-PH domains of Sos form an L-shaped structure in which two distinct structural modules, with distinct hydrophobic cores, are clearly delineated (Figure 3). The

in these areas. Secondary structure elements corresponding to the Sos structure are depicted as bars for α helices, arrows for β sheets, and lines for coil regions. The disordered linker between the two domains is shown as a dotted line. Secondary structure elements corresponding to the Dbl homology domain (residues 198–404) are colored blue, and those corresponding to the pleckstrin homology domain (residues 442–550) are colored yellow. The linker segment (residues 405–441), which includes the disordered interdomain linker (residues 405–417) as well as the N-terminal extension of the PH domain (residues 418–442), is colored red. The conserved regions (CR) of the DH domain are marked with colored lines and text (magenta, CR1; peach, CR2; olive green, CR3).

Table 1. Data Collection and Refinement Statistics

MAD Phasing				
Energies (eV)	No. of Reflections (Total/Unique)	Completeness (%)	Overall I/σ(I) (%)	R_{sym}
λ_1 12580	238,642/23,805	98.9 (96.9)	21.1	3.6 (18.7)
λ_2 12660	239,135/23,828	98.9 (96.9)	20.3	3.8 (20.6)
λ_3 12662	238,877/23,798	98.9 (96.9)	19.5	4.1 (22.4)
λ_4 12800	241,156/24,007	98.7 (96.7)	19.9	3.8 (22.0)
Mean overall figure of merit (30.0–2.3 Å) (centric/acentric) = 0.58/0.66.				

Refinement and Stereochemical Statistics (All Data 30.0–2.3 Å)	
R value	22.6%
Free R value	26.8%
Average B factors	(Å^2)
Protein	41.4 (34.2 DH domain, 53.4 PH domain)
Solvent	38.1
Rms deviations	
Bonds (Å)	0.0066
Angles (°)	1.257

$R_{sym} = 100 \times \Sigma|I - <I>|/\Sigma I$, where I is the integrated intensity of a given reflection. For R_{sym} and completeness, numbers in parentheses refer to data in the highest resolution shell.
Figure of merit = $< | \Sigma P(\alpha) e^{i\alpha} / \Sigma P(\alpha) | >$, where α is the phase and $P(\alpha)$ is the phase probability distribution.
R value = $\Sigma| F_p - F_p(\text{calc}) | / \Sigma F_p$, where F_p is the structure factor amplitude. The free R value is the R value for a 10% subset of the data that was not included in the crystallographic refinement.

first module, or structural domain, spans residues 198–404 and is the architectural unit we shall refer to as the DH domain. The second structural domain, consisting of residues 418–550, includes the boundaries of the conventional PH domain (residues 443–550), as well as 24 residues (418–442) that have been considered part of the DH domain on the basis of sequence comparisons. The NMR structures of the isolated PH domains from human and mouse Sos1 showed that residues 422–442 of the conventional DH domain form a structure that is integrated into the PH domain (Koshiba et al., 1997; Zheng et al., 1997). Our results now demonstrate that this segment is not part of the structural unit corresponding to the DH domain. Residues 405–417, which connect the C terminus of the DH structural domain to the N-terminal extension of the PH domain, are disordered. Electron density for this region is completely absent, and SDS-PAGE analysis of the crystals demonstrates that the polypeptide chain of the DH-PH construct is intact (data not shown). The flexible interdomain linker and the N-terminal extension of the PH domain shall be referred to collectively as the linker segment (colored red in Figures 1, 2, 3, and 5). Even though the interdomain linker is disordered, an examination of the crystal packing interactions reveals that the structure presented here is the only combination of DH and PH domains in the crystal lattice that can be joined by the 13-residue interdomain linker. The two domains form the most extensive interface observed between any DH and PH domains in the crystal lattice, further suggesting that this is the relevant DH-PH structure for Sos.

The Dbl Homology Domain

The DH domain of Sos contains 11 helical segments, denoted H1-H11, which fold into an oblong helical bundle (Figures 1 and 3). Three of the helical segments are interrupted by kinks, and the two distinct helices in each of these segments are denoted a and b, respectively. DH domains contain three highly conserved blocks of sequence that have been referred to previously as conserved regions 1–3, or CR1-3 (Figure 1 and (Boguski and McCormick, 1993; Whitehead et al., 1997)). These three conserved regions form three long helices, H1a, H2b, and H8, which pack together to form the core of the DH domain (Figure 3). The H1a helix (CR1) leads into a sharp helical hairpin that is formed by helices H1b and H2a. This hairpin is followed by another long helix, H2b (CR2), which packs against the H1a helix. The H3 and H4 helices interact with one face of the H2b helix and lead into a U-shaped arrangement of the H5, H6, and H7a helices. This block of helices stacks against one face of the helical hairpin formed by H1b and H2a and serves as a structural scaffold upon which the PH domain is situated. The short H7b helix leads into the longer H8 helix (CR3) and is followed by the H9, H10, and H11 helices, which terminate the DH domain on the convex surface formed by the H1a, H8, and H9 helices (Figure 3).

Searches of the structural database using DALI (Holm and Sander, 1993) failed to reveal any structure with a fold similar to that of the DH domain, and there is no obvious relationship between the fold of the DH domain and that of other nucleotide exchange factors of known structure. The fact that the three highly conserved regions of the DH domain (CR1, CR2, and CR3) pack together to form the central core of the structure argues strongly that other DH domains will have a very similar overall construction. Interestingly, the Sos DH domain deviates in sequence from other DH domains at several positions. For example, Ile-212 in CR1 of Sos is a glutamic acid in every other protein (Figure 1). Other differences are also found in the CR2 and CR3 regions of Sos. The functional consequences of these variations in CR1, CR2, and CR3 are not known, and modeling studies (data not shown) indicate that these differences

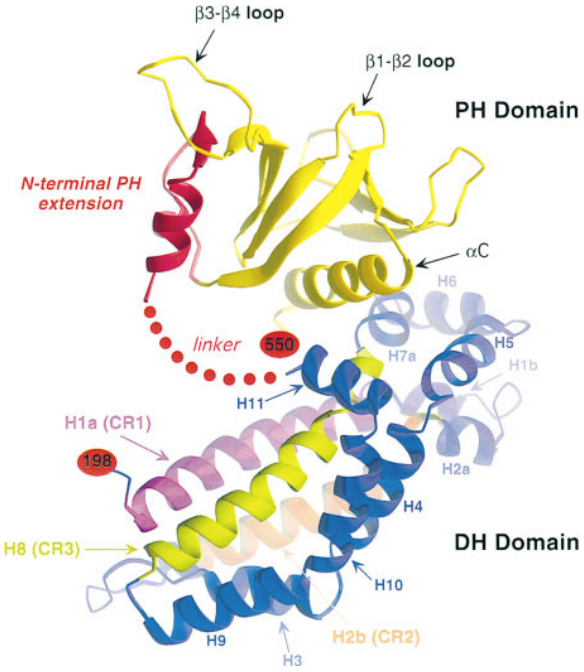

Figure 3. Ribbon Diagram of the Structure of the DH and PH Domains from Sos

All ribbon diagrams were generated using the program RIBBONS (Carson, 1991). Coloring is as depicted in Figure 1; the DH domain is blue, the PH domain is yellow, and the linker segment is red. The conserved regions of the DH domain are labeled and colored as in Figure 1. Magenta, CR1; peach, CR2; olive green, CR3. Red ovals mark the amino- and carboxyl-terminal residues of the DH-PH domains (residues 198 and 550, respectively).

between the Sos sequence and the general DH consensus sequence should not result in significant structural differences in the structure of the core DH domain.

Interactions between the DH and PH domains occur primarily between helix αC of the PH domain (residues 531–545) and helix H7a (residues 331–337) of the DH domain (Figure 3). The interface consists of both tight hydrophobic packing and specific hydrogen bonding interactions and buries a total surface area of around 1,100 Å^2. Surprisingly, the regions of the DH and PH domains that form the interface are among the most poorly conserved regions of the molecule (Figure 1). The most variable regions of the DH domain cluster at one end of the molecule, in the small helical bundle formed by helices H1b, H2b, H5, H6, and H7a (Figure 3). These helices position helix H7a appropriately for interaction with the PH domain. Particularly striking is the extreme variability in the sequences of DH domains in the region corresponding to helix H7a of Sos (Figure 1). Likewise, most of the residues in helix αC of the PH domain that contact the DH domain (residues 535, 536, 538, 539, 542, 543, 546, 549, and 550) are extremely variable among Dbl family members (Figure 1). The sequence diversity observed in this clustered region of the structure is suggestive of structural variation in the DH family that may affect the manner in which the DH and PH domains associate.

The surface of the DH domain contains only one contiguous patch of highly conserved residues (Figure 4). Residues on this conserved surface are contributed primarily from helices H1a and H8, which comprise CR1 and CR3, respectively (Figures 3 and 4). Nearly all of the amino acid substitutions known to affect DH function map to this conserved region of the molecular surface. For instance, the replacement of residues ^{640}LLLKELL^{646} of Dbl (residues 355–361 of Sos in CR3), by the sequence IIIRDII, causes Dbl to lose its transforming ability (Ron et al., 1991) and also abolishes exchange factor activity (Hart et al., 1994). Likewise, substitution of the corresponding region of the RasGRF DH domain, ^{390}ITLHELL^{396}, with IIIRDII, abrogates RasGRF responsiveness to calcium (Freshney et al., 1997). An overlapping cluster of mutations in the mouse Sos1 DH domain, ^{351}LHYFELL^{357}, mutated to IIIRDII, significantly reduces the transforming capability of Sos (Qian et al., 1998). Similarly, the single substitution of Leu-321 to glutamic acid (residue 356 in Sos) abolishes mouse Net1 exchange factor activity (Alberts and Treisman, 1998). The mutation of Ser^{1216} to Phe (residue 211 in Sos) abolishes in vitro exchange factor activity of Unc73 toward Rac and results in a characteristic uncoordinated phenotype in *C. elegans* (Steven et al., 1998). This mutation lies on helix H1a (CR1), adjacent to the previous mutations described on helix H8 (CR3), and is part of the contiguous patch of conserved surface residues (Figures 3 and 4).

Taken together, the sequence conservation analysis and mutation data strongly support the conclusion that the conserved region of the molecular surface is critical for DH domain functionality. In particular, the results with Dbl, Net1, and Unc73 demonstrate clearly that this surface is involved in GTPase binding and nucleotide exchange factor activity. It should, however, be noted that the mutations in mouse Sos1 and RasGRF described above have not been linked directly to DH-catalyzed nucleotide exchange factor activity and may reflect the ability of the DH domain to participate in other inter- and intramolecular regulatory interactions, as has been previously suggested (Freshney et al., 1997; Corbalan-Garcia et al., 1998; Qian et al., 1998).

There is no overall correlation between the structure of the Ras exchange factor region of Sos (Boriack-Sjodin et al., 1998) and that of the DH-PH domains described here. There is, however, a possible similarity between certain features at the active sites of the two exchange factor regions. There are two key elements to the interaction between Ras and the Ras exchange factor region of Sos. First, an α helix from Sos (helix αH) is inserted into the catalytic site of Ras, resulting in the expulsion of the so-called Switch 1 region of Ras from the vicinity of the nucleotide and the occlusion of the binding sites for the phosphates of the nucleotide and the associated magnesium ion by acidic and hydrophobic side chains. Second, the N-terminal region of helix αH in Sos is so arranged that an exposed hydrophobic pocket is formed at the point where it intersects two other helices (αB and αD). This hydrophobic pocket is the central anchor point for Ras, since it forms a binding site for hydrophobic residues from the Switch 2 region of Ras. Of these, Tyr-64 and Met-67 of Ras appear to be particularly important.

Many of the mutations that diminish the nucleotide exchange activity of DH domains are located on helix

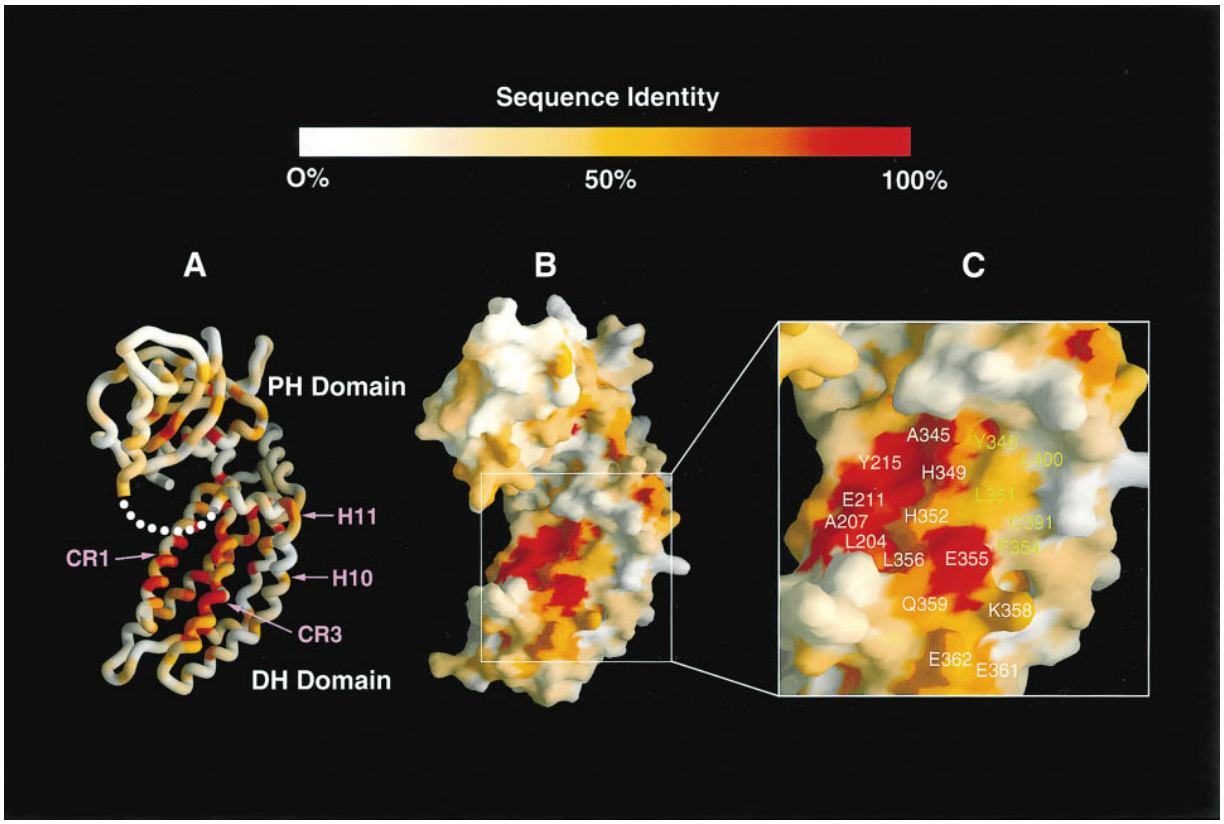

Figure 4. Identification of the Putative Active Site Region of the DH Domain

Sequence conservation depicted in Figure 1 mapped onto the protein backbone worm (A) and surface (B). Sequence identity from 0%–100% is presented as a color gradient from white to yellow to red. A magnified view of the highly conserved region of the molecular surface is shown (C) with residue numbers corresponding to Sos numbering (see Figure 1). Labels for residues that form the hydrophobic pocket discussed in the text are colored green. Figure prepared using GRASP (Nicholls et al., 1991).

H8 (CR3), which is the most highly conserved region of the DH domains (Figures 1, 3, and 4). The exposed surface of helix H8, like that of helix αH of the Ras exchange factor region of Sos, includes a mixture of hydrophobic and charged residues. As in the Ras exchange factor domain, the base of helix H8 of the DH domain is arranged so that an exposed hydrophobic pocket is formed in the region where H8 intersects H10 and H11. Residues Tyr-348, Leu-351, Phe-354, Cys-391, and Leu-400 of the DH domain line the hydrophobic pocket (Figure 4). By analogy to the Ras/Sos structure, it is possible that this pocket serves as an anchor point for the Switch 2 region of the incoming GTPase, with helix H8 (CR3) playing a key role in disrupting the nucleotide binding site.

The Pleckstrin Homology Domain

The structure of the Sos PH domain, presented here in the context of the DH domain, is very similar to the NMR structures of the isolated human and mouse Sos PH domains determined in solution (Koshiba et al., 1997; Zheng et al., 1997). For example, the crystal structure and the NMR structures of the human Sos PH domain superimpose with an overall root-mean-square difference (rmsd) in α carbon positions of 3.5 Å, and only 1.6 Å if loop regions are omitted. As observed in the NMR structure of the human Sos PH domain (Zheng et al., 1997), residues 418–442 form an N-terminal extension of the PH domain that folds into a structure consisting of an α helix (αN), a short β strand (βN), and a turn of 3/10 helix (Figure 5A). These elements pack against one face of the β sheet formed by strands β1–β4 and interact with one edge of the β3-β4 loop. Despite poor sequence conservation in the N-terminal extension of the PH domain (Figure 1), it has been postulated that other DH-associated PH domains may have similar structures, since the portions of these sequences corresponding to αN are all predicted to have high helix-forming probabilities (Zheng et al., 1997).

The PH domains of Sos and Vav have been reported to bind phospholipids in vitro with varying affinities and specificities (Chen et al., 1997; Koshiba et al., 1997; Kubiseski et al., 1997; Rameh et al., 1997; Zheng et al., 1997; Han et al., 1998). Phospholipids appear to modulate the activity of the Sos and Vav DH domains, indicating that phospholipid binding is a functionally important property of these PH domains (Han et al., 1998; Ma et al., 1998; Nimnual et al., 1998). The structure of the liganded form of the PH domain of Sos is not known; however, chemical shift perturbation has shown that the binding site for inositol (1,4,5)-triphosphate is located in the pocket between the β1-β2 and β3-β4 loops (Koshiba et al., 1997; Zheng et al., 1997). The

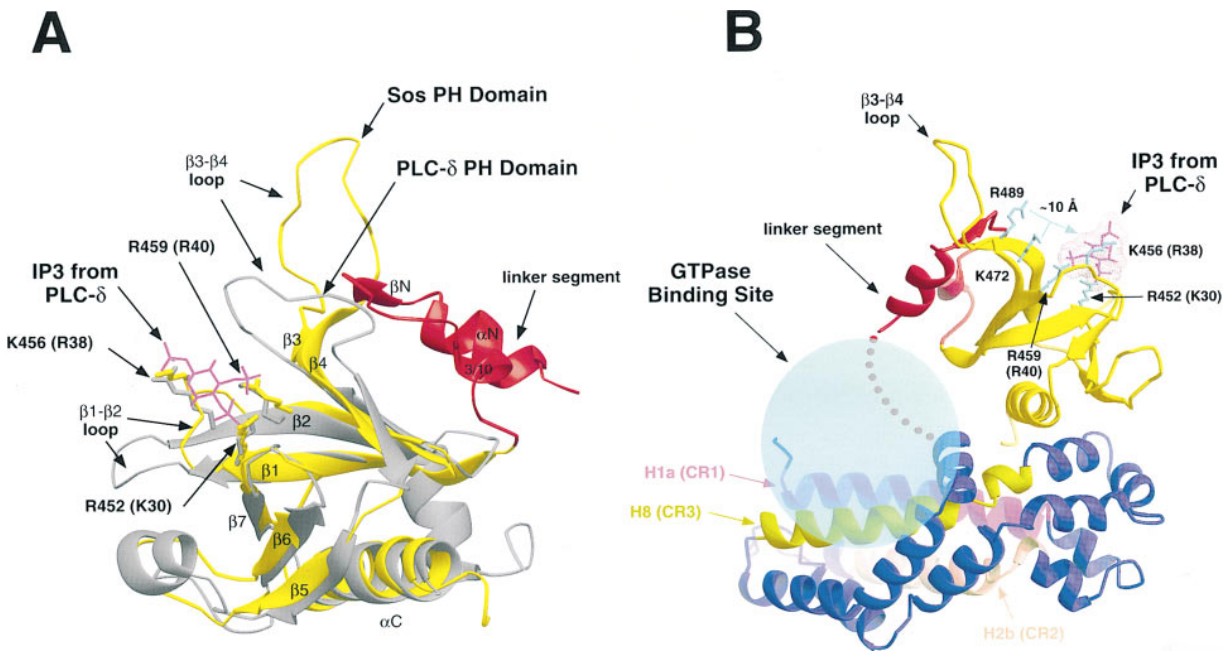

Figure 5. The Sos PH Domain and Possible Mechanism for DH Regulation by Phospholipid Binding

(A) Ribbon diagram of the crystal structure of the PH domain of Sos, viewed in an orientation rotated by 180° about the vertical with respect to Figure 3. The core PH domain of Sos (residues 442–550) is colored yellow, while the unique N-terminal extension of the PH domain (residues 418–442) is colored red. The crystal structure of the Sos PH domain was superimposed with the crystal structure of the PH domain from phospholipase C-δ (gray ribbon) in complex with inositol (1,4,5) triphosphate (magenta ball-and-stick representation) (Ferguson et al., 1995) using the program O (Jones et al., 1991). Secondary structure elements are labeled, and positions of the β1-β2 and β3-β4 loops that are involved in ligand binding are marked with text and arrows. The three positively charged side chains that contact the sugar phosphates from PLC-δ are colored gray, and the corresponding side chains from Sos are colored yellow. Residues are labeled relative to Sos numbering with the PLC-δ numbers in parentheses.

(B) The structural connection between the phospholipid binding site and the GTPase binding site. Structural elements are labeled and colored as in previous figures. The area occupied by the bound GTPase, as inferred from the location of the binding site, is colored as a translucent cyan circle. Side chains from Sos that are implicated in inositol phosphate binding are colored cyan and labeled as in (A).

location of this binding site is very similar to that observed in the structure of the liganded form of the PH domain from phospholipase C-δ (PLC-δ) (Ferguson et al., 1995), suggesting that the overall features of binding will be similar between the two proteins. The Sos and PLC-δ PH domains share only 11% sequence identity, but superposition of the PLC-δ and Sos PH domains, excluding the variable loop regions, yields an rmsd in α carbon positions of 1.7 Å (Figure 5A). Strikingly, three basic residues that make direct contacts to the sugar phosphates in the PLC-δ complex (Lys-30, Arg-38, and Arg-40) are conserved both in sequence location and in three-dimensional structure in the Sos PH domain (Arg-452, Lys-456, and Arg-459; see Figure 5A). Two of these residues, Lys-456 and Arg-459, exhibit significant backbone chemical shifts upon ligand binding (Zheng et al., 1997). Mutation of these same two residues decreases the affinity for phosphatidylinositol (4,5)-bisphosphate (Chen et al., 1997; Kubiseski et al., 1997), providing further evidence that the mode of ligand binding will be similar between the Sos and PLC-δ PH domains.

The PH domain in the DH-PH unit is oriented so that one wall of the probable GTPase binding site is formed by the surface of the PH domain that is distal to the phospholipid binding site (Figure 5B). The N-terminal linker segment of the PH domain is part of this distal surface, and it is connected to the β3-β4 loop through the formation of a β sheet that includes strands βN (of the linker segment) and strands β3-β4 of the PH domain. Comparison of the structure of the unliganded form of the Sos PH domain seen here with that of the liganded form of the PH domain of PLC-δ suggests that ligation of the PH domain will result in structural changes in the β3-β4 loop and the linker segment of the Sos PH domain. Supporting this hypothesis, backbone chemical shifts are observed upon ligand binding for two residues in the base of the β3-β4 loop, Arg-489 and Lys-472 (Zheng et al., 1997). The unliganded structure presented here shows that the side chains of these residues are located approximately 10 Å from the inositol phosphate binding site, implying a significant change in conformation of the β3-β4 loop upon ligand binding. As postulated previously, a structural change in the β3-β4 loop would alter the conformation of the N-terminal extension of the PH domain (Zheng et al., 1997). Our structure suggests that these ligand-induced structural changes in the PH domain are likely to affect the interaction of the DH domain with GTPases, as a consequence of their location adjacent to the proposed GTPase binding site (Figure 5B).

Conclusions

The structure of the DH-PH domains from Sos reveals the architecture of the Dbl-homology guanine nucleotide

exchange factor for Rho-family GTPases. The degree and pattern of sequence conservation suggests that the core structure of the DH domain is likely to be preserved among all Dbl-family members. A highly conserved region of the molecular surface harbors many residues that when mutated abolish DH domain function, suggesting that this region is responsible for GTPase binding and nucleotide exchange factor activity. The structure also reveals how the DH domain of Sos interacts with its tandem PH domain and that the regions of the molecule involved in this interaction are among the most poorly conserved regions of the Dbl family. This suggests, somewhat surprisingly, that the manner in which the DH and PH domains associate may not be conserved in other members of the family. The relative disposition of the PH domain and the DH domain active site in Sos suggests that ligand binding to the PH domain could regulate the interaction of the DH domain with its target GTPase. Future studies will hopefully shed light on the role of the PH domain of Sos, and other Dbl family members, in regulating Rho GTPase exchange factor activity. The structure presented here lays the groundwork for the elucidation of the mechanism of DH-catalyzed nucleotide exchange and the regulatory mechanisms governing this important class of proteins.

Experimental Procedures

Preparation and Crystallization of the Sos DH-PH Construct

A fragment of Sos corresponding to residues 180–551, plus an N-terminal six-histidine affinity tag, was produced in *Escherichia coli* using a tac expression system and purified using standard Ni-affinity procedures. A stable subfragment of residues 189–551 was identified on the basis of resistance to elastase digestion, coupled with mass spectroscopy and N-terminal peptide sequencing (data not shown). DNA corresponding to this fragment was subcloned into a pPROEX-HT expression vector (Life Technologies). Preparative scale growth of this protein fragment was done in 8 l of BL21 cells grown to an A_{600} of 0.7 at 37°C in standard Luria Broth with 200 μg/ml ampicillin. The temperature was reduced to 30°C, and IPTG was added to a concentration of 0.5 mM to induce protein expression. Cells were grown for an additional 4–5 hr, harvested by centrifugation, resuspended in lysis buffer (10 mM Tris [pH 8.0], 200 mM NaCl) and frozen at −80°C. Cells were thawed, and 1 mM PMSF and 5 mM 2-mercaptoethanol were added prior to lysis using an Emulsiflex French press (Avestin) in three passes at a pressure of 10,000 lb/in^2, followed by centrifugation at 14,000 rpm in an SS-34 rotor to pellet cell debris. The clarified lysate was passed through a 0.45 micron filter and the histidine-tagged fragment of Sos was isolated using a Ni-NTA (Qiagen) column. After cleavage with TEV protease, the protein was flowed through the Ni-NTA column to remove uncleaved fusion protein, followed by purification over a HiQ column (BioRad). Pooled HiQ fractions were concentrated to approximately 1 ml and loaded onto a Superdex S75 column (Pharmacia) equilibrated in 20 mM Tris (pH 8.0), 1 mM EDTA, 200 mM NaCl, and 1 mM DTT. Peak fractions were concentrated to approximately 10 mg/ml and flash frozen in liquid nitrogen for long-term storage at −80°C. The average yield was around 10 mg of purified DH-PH protein per liter of culture. Crystals were grown using sitting drop vapor diffusion by mixing equal volumes of a 5 mg/ml protein solution and 1%–3% PEG 6000 (Fluka) and 100 mM Bis-Tris (pH 6.5) and then equilibrating over a 750 μl reservoir of the same buffer at 20°C. Crystals grow to an average size of 0.3 mm × 0.3 mm × 0.05 mm in about 1 week. Selenomethionine-substituted protein was prepared by expressing protein in the methionine auxotrophic strain JB(DE3). Cells were grown overnight in LB media and then amplified in M9 minimal media supplemented with 0.4 g/l threonine and serine, and 0.03 g/l of phenylalanine, leucine, isoleucine, valine, lysine, arginine, histidine, aspartic acid, glutamic acid, tyrosine, and tryptophan. L-selenomethionine (Calbiochem) was added to a final concentration of 25 mg/l, followed by 1 mM $MgSO_4$, 0.0005% (w/v) thiamine, 0.2% glucose, and 20 mM $CaCl_2$. Cells were induced with IPTG as described above and grown for 6.5 hr prior to harvesting. Selenium incorporation was verified using high-resolution electrospray ionization mass spectrometry (data not shown). Purification and crystallization proceeded as described for the native protein.

Data Collection and Structure Solution

Crystals of the Sos DH-PH domains were harvested into a stabilization buffer of 5% PEG 6000 and 100 mM Bis-Tris. The crystals were transferred to stabilization buffer plus 17% glycerol for approximately 3 min and then into stabilization buffer plus 34% glycerol. Crystals were immediately frozen in liquid nitrogen cooled liquid propane for later use in data collection. All data were integrated and reduced with the DENZO/SCALEPACK programs (Otwinowski and Minor, 1997), while subsequent manipulations were performed using the CCP4 suite of programs (CCP4, 1994). Crystals form in space group C2 with unit cell dimensions of a = 104.4 Å, b = 70.4 Å, c = 73.8 Å, β = 96.3° and contain one DH-PH molecule in the asymmetric unit with a solvent content of approximately 60%. A mercury derivative was prepared by soaking the crystals in stabilization buffer with 0.1 mM thimerasol for 2 hr. A low-resolution data set was collected on this derivative, and phases calculated using MLPHARE (CCP4) were used in cross-difference Fourier maps to locate seven of the nine possible selenium atoms in the selenomethionyl-substituted protein. The handedness of the heavy atom sites was determined at this time by inspecting 4 Å resolution MIR maps calculated with the thimerasol and selenium sites in both possible hands. Clear electron density for several long helices in the DH domain defined the hand of the heavy atom sites unambiguously. Multiwavelength anomalous dispersion (MAD) data were collected from the selenomethionyl-derivatized crystals at four wavelengths around the K absorption edge of selenium at beamline X4A of the National Synchrotron Light Source (Brookhaven, NY) (Table 1). Data were measured over a full 360° rotation of the crystal, in 10° wedges of reciprocal space using inverse beam geometry, interleaving the four wavelengths. The scaled and reduced intensity data were then converted to amplitudes using TRUNCATE (CCP4), and cross wavelength scaling was performed using SCALEIT (CCP4), treating λ_2 (Table 1) as the native. The anomalous data were treated as a special case of multiple isomorphous replacement as previously described (Ramakrishnan and Biou, 1997). Phase calculation and heavy atom refinement using MLPHARE resulted in a final overall figure of merit from 30 to 2.3 Å of 0.65. Automated solvent flattening using DM (CCP4) resulted in an electron density map of exceptional quality (data not shown), into which a nearly complete model was built using O (Jones et al., 1991). Refinement of the model by CNS (Brünger et al., 1998) utilized the λ_1 selenomethionine data set (Table 1), with the maximum likelihood target function (Pannu and Read, 1996). Corrections for the bulk solvent and for anisotropy in the data were applied after the first two rounds of refinement. σ_a weighting schemes (Read, 1986), as implemented in CNS, were used throughout for map calculations. Waters were conservatively added to peaks of F_o-F_c density greater than 3σ and that were making at least one hydrogen bond to the protein or another already placed water molecule. All water molecules in the final model have B factors less than 60 Å^2. The final refined model, at 2.3 Å resolution, has a crystallographic R value of 22.6%, a free R value of 26.8% (22.5% and 26.6%, respectively, for reflections with $|F| > 2\sigma|F|$), and consists of residues 198–550 of the Sos DH-PH domains and 69 water molecules. Electron density for the residues comprising the linker between the DH and PH domains (residues 405–417) is lacking, and these residues were not included in the final model. The model has excellent stereochemistry, and analysis with PROCHECK (Laskowski et al., 1993) yields scores better than average in all categories when compared to structures determined at similar resolution. The Ramachandran plot has 94% of the residues lying in the most-favored regions and no residues in disallowed regions.

Structure Analysis

The following 20 sequences were aligned (Figure 1) using CLUSTALW-1.6 (Higgins et al., 1991): human Sos1 (h_sos1), human

Dbl (h_dbl), *C. elegans* unc-73 (unc-73), human Abr (h_abr), human Bcr (h_bcr), human Fgd1 (h_fgd1), human Lbc (h_lbc), human Net1 (h_net1), human Tiam-1 (h_tiam1), human Trio1 (h_trio1), human Trio2 (h_trio2), mouse Dbs (m_Dbs), mouse Ect2 (m_ect2), mouse Lfc (m_lfc), mouse Lsc (m_lsc), mouse RasGRF (m_rasgrf), mouse Vav (m_vav), rat Ost (r_ost), *S. cerevisiae* cdc24 (sc_cdc24), *S. pombe* Scd1 (sp_scd1). For proteins where sequences from more than one species are present in the database, only one sequence was included in the alignment so as not to overly bias subsequent calculations. The percent identity of the most commonly occurring residue at every position in the CLUSTALW alignment was calculated, and this percentage was used to color code residues and surfaces using the program GRASP (Nicholls et al., 1991).

Acknowledgments

We are grateful to C. Ogata of beamline X4A for advice on data collection and processing, and to J. Bonanno, T. Schindler, and H. Yamaguchi for assistance with synchrotron data collection. Beamline X4A at the National Synchrotron Light Source, a DOE facility, is supported by the Howard Hughes Medical Institute. We also thank T. Muir for assistance with electrospray mass spectroscopy, D. Leahy for useful discussions on MAD phasing, and A. Boriack-Sjodin, S. K. Burley, X. Chen, E. Conti, M. Huse, D. Jeruzalmi, B. A. Yatzula, and Y. Zhang for advice and help. S. M. S. is supported by the Cancer Research Fund of the Damon Runyon-Walter Winchell Foundation Fellowship (DRG 1494), and A. S. N. is supported by National Institutes of Health training grant CA09176. D. B.-S. acknowledges support by National Institutes of Health grants CA28146 and CA55360. Coordinates will be deposited with the Brookhaven Protein Data Bank. Prior to release, the coordinates may be obtained at the website (http://www.rockefeller.edu/kuriyan).

Received July 29, 1998; revised August 27, 1998.

References

Alberts, A.S., and Treisman, R. (1998). Activation of RhoA and SAPK/JNK signaling pathways by the RhoA-specific exchange factor mNet1. EMBO J. *17*, 4075–4085.

Bar-Sagi, D. (1994). The Sos (Son of sevenless) protein. Trends Endocrinol. Metab. *5*, 165–169.

Boguski, M.S., and McCormick, F. (1993). Proteins regulating Ras and its relatives. Nature *366*, 643–654.

Boriack-Sjodin, P.A., Margarit, S.M., Bar-Sagi, D., and Kuriyan, J. (1998). Structural basis of the activation of Ras by Sos. Nature *394*, 337–343.

Bourne, H.R., Sanders, D.A., and McCormick, F. (1991). The GTPase superfamily: conserved structure and molecular mechanism. Nature *349*, 117–127.

Brünger, A.T., Adams, P.D., Clore, G.M., DeLano, W.L., Gros, P., Grosse-Kunstleve, R.W., Jiang, J.-S., Kuszewski, J., Nilges, M., Pannu, N.S., et al. (1998). Crystallography and NMR system (CNS): a new software suite for macromolecular structure determination. Acta Crystallogr., in press.

Carson, M. (1991). Ribbons 2.0. J. Appl. Crystallogr. *24*, 958–961.

CCP4 (1994). Collaborative Computing Project No. 4. The CCP4 suite: programs for protein crystallography. Acta Crystallogr. *D50*, 760–763.

Cerione, R.A., and Zheng, Y. (1996). The Dbl family of oncogenes. Curr. Opin. Cell Biol. *8*, 216–222.

Chen, R.-H., Corblan-Garcia, S., and Bar-Sagi, D. (1997). The role of the PH domain in the signal-dependent membrane targeting of Sos. EMBO J. *16*, 1351–1359.

Cherfils, J., Ménétrey, J., Mathieu, M., Bras, G.L., Robineau, S., Béraud-Dufour, S., Antonny, B., and Chardin, P. (1998). Structure of the Sec7 domain of the Arf exchange factor ARNO. Nature *392*, 101–105.

Corbalan-Garcia, S., Margarit, S.M., Galron, D., Yang, S.-S., and Bar-Sagi, D. (1998). Regulation of Sos activity by intramolecular interactions. Mol. Cell. Biol. *18*, 880–886.

Coso, O., Chiariello, M., Yu, J.-C., Teramoto, H., Crespo, P., Xu, N., Miki, T., and Gutkind, J.S. (1995). The small GTP-binding proteins Rac1 and Cdc42 regulate the activity of the JNK/SAPK signaling pathway. Cell *81*, 1137–1146.

Eva, A., and Aaronson, S.A. (1985). Isolation of a new human oncogene from a diffuse B-cell lymphoma. Nature *316*, 273–275.

Ferguson, K.M., Lemmon, M.A., Schlessinger, J., and Sigler, P.B. (1995). Structure of the high affinity complex of inositol trisphosphate with a phospholipase C pleckstrin homology domain. Cell *83*, 1037–1046.

Freshney, N.W., Goonesekera, S.D., and Feig, L.A. (1997). Activation of the exchange factor Ras-GRF by calcium requires an intact Dbl homology domain. FEBS Lett. *407*, 111–115.

Habets, G.G.M., Scholtes, E.H.M., Zuydgeest, D., Kammen, R.A.v.d., Stam, J.C., Berns, A., and Collard, J.G. (1994). Identification of an invasion-inducing gene, *Tiam-1*, that encodes a protein with homology to GDP-GTP exchangers for Rho-like proteins. Cell *77*, 537–549.

Hall, A. (1998). Rho GTPases and the actin cytoskeleton. Science *279*, 509–514.

Han, J., Luby-Phelps, K., Das, B., Shu, X., Xi, Y., Mosteller, R.D., Krishna, U.M., Falck, J.R., White, M.A., and Broek, D. (1998). Role of substrates and products of PI 3-kinase in regulating activation of Rac-related guanosine triphosphatases by Vav. Science *279*, 558–560.

Hart, M.J., Eva, A., Evans, T., Aaronson, S.A., and Cerione, R.A. (1991). Catalysis of guanine nucleotide exchange on the CDC42Hs protein by the *dbl* oncogene product. Nature *354*, 311–314.

Hart, M.J., Eva, A., Zangrilli, D., Aaronson, S.A., Evans, T., Cerione, R.A., and Zheng, Y. (1994). Cellular transformation and guanine nucleotide exchange activity are catalyzed by a common domain on the *dbl* oncogene product. J. Biol. Chem. *269*, 62–65.

Higgins, D.G., Bleasby, A.J., and Fuchs, R. (1991). CLUSTALV: improved software for multiple sequence alignment. Cabios *8*, 189–191.

Hill, C.S., Wynne, J., and Treisman, R. (1995). The Rho family GTPases RhoA, Rac1, and Cdc42Hs regulate transcriptional activation by SRF. Cell *81*, 1159–1170.

Holm, L., and Sander, C. (1993). Protein structure comparison by alignment of distance matrices. J. Mol. Biol. *233*, 15511–15519.

Jones, T.A., Zou, J.Y., Cowen, S.W., and Kjeldgaard, M. (1991). Improved methods for building protein models in electron density maps and the location of errors in these models. Acta Crystallogr. *A47*, 110–119.

Kawashima, T., Berthet-Colominas, C., Wulff, M., Cusack, S., and Leberman, R. (1996). The structure of *Escherichia coli* Ef-Tu/Ef-Ts complex at 2.5 Å resolution. Nature *379*, 511–518.

Konishi, H., Kuroda, S., Tanaka, M., Matsuzaki, H., Ono, Y., Kameyama, K., Haga, T., and Kikkawa, U. (1995). Molecular cloning and characterization of a new member of the RAC protein kinase family: association of the pleckstrin homology domain of three types of RAC protein kinase with protein kinase C subspecies and $\beta\gamma$ subunits of G-proteins. Biochem. Biophys. Res. Commun. *216*, 526–534.

Koshiba, S., Kigawa, T., Kim, J.-H., Shirouza, M., Botwell, D., and Yokoyama, S. (1997). The solution structure of the pleckstrin homology domain of mouse Son-of-sevenless 1 (mSos1). J. Mol. Biol. *269*, 579–591.

Kubiseski, T.J., Chook, Y.M., Parris, W.E., Rozakis-Adcock, M., and Pawson, T. (1997). High affinity binding of the pleckstrin homology domain of mSos1 to phosphatidylinositol (4,5)-bisphosphate. J. Biol. Chem. *272*, 1799–1804.

Laskowski, R.A., MacArthur, M.W., Moss, D.S., and Thornton, J.M. (1993). PROCHECK: a program to check the stereochemical quality of protein structures. J. Appl. Crystallogr. *26*, 283–291.

Lemmon, M.A., and Ferguson, K.M. (1998). Pleckstrin homology domains. Curr. Topics Microbiol. Immunol. *228*, 39–74.

Lenzen, C., Cool, R.H., Prinz, H., Kuhlmann, J., and Wittinghofer, A. (1998). Kinetic analysis by fluorescence of the interaction between

Ras and the catalytic domain of the guanine nucleotide exchange factor Cdc25^{Mm}. Biochemistry *37*, 7420–7430.

Ma, A.D., Metjian, A., Bagrodia, S., Taylor, S., and Abrams, C.S. (1998). Cytoskeletal reorganization by G protein-coupled receptors is dependent on phosphoinositide 3-kinase γ, a Rac guanosine exchange factor, and Rac. Mol. Cell. Biol. *18*, 4744–4751.

Minden, A., Lin, A., Claret, F.-X., Abo, A., and Karin, M. (1995). Selective activation of the JNK signaling cascade and c-Jun transcriptional activity by the small GTPases Rac and Cdc42Hs. Cell *81*, 1147–1157.

Mossessova, E., Gulbis, J.M., and Goldberg, J. (1998). Structure of the guanine nucleotide exchange factor Sec7 domain of human Arno and analysis of the interaction with ARF GTPase. Cell *92*, 415–423.

Nicholls, A., Sharp, K.A., and Honig, B. (1991). Protein folding and association: insights from the interfacial and thermodynamic properties of hydrocarbons. Proteins: Struct. Func. Genet. *11*, 281–296.

Nimnual, A.S., Yatsula, B.A., and Bar-Sagi, D. (1998). Coupling of the Ras and Rac guanosine triphosphatases through the Ras exchanger Sos. Science *279*, 560–563.

Olson, M.F., Ashworth, A., and Hall, A. (1995). An essential role for Rho, Rac, and Cdc42 GTPases in cell cycle progression through G1. Science *269*, 1270–1272.

Otwinowski, Z., and Minor, W. (1997). Processing of x-ray diffraction data collected in oscillation mode. Methods Enzymol. *276*, 307–326.

Pannu, N.S., and Read, R.J. (1996). Improved structure refinement through maximum likelihood. Acta Crystallogr. *A52*, 659–668.

Pitcher, J.A., Touhara, K., Payne, E.S., and Lefkowitz, R.J. (1995). Pleckstrin homology domain-mediated membrane association and activation of the β-adrenergic receptor kinase requires coordinate interaction with Gβγ subunits and lipid. J. Biol. Chem. *270*, 11707–11710.

Qian, X., Vass, W.C., Papageorge, A.G., Anborgh, P.H., and Lowy, D.R. (1998). N terminus of Sos1 Ras exchange factor: critical roles for the Dbl and pleckstrin homology domains. Mol. Cell. Biol. *18*, 771–778.

Qiu, R.-G., Chen, J., Kirn, D., McCormick, F., and Symons, M. (1995). An essential role for Rac in Ras transformation. Nature *374*, 457–459.

Raabe, T. (1998). Genetic analysis of Sevenless tyrosine kinase signaling in *Drosophila*. Curr. Topics Microbiol. Immunol. *228*, 343–361.

Ramakrishnan, V., and Biou, V. (1997). Treatment of multiwavelength anomalous diffraction data as a special case of multiple isomorphous replacement. Methods Enzymol. *276*, 538–557.

Rameh, L.E., Arvidsson, A.-k., Carraway, III, K.L., Couvillon, A.D., Rathbun, G., Crompton, A., VanRenterghem, B., Czech, M.P., Ravichandran, K.S., Burakoff, S.J., Wang, D.-S., Chen, C.-S., and Cantley, L.C. (1997). A comparative analysis of the phosphoinositide binding specificity of pleckstrin homology domains. J. Biol. Chem. *272*, 22059–22066.

Read, R.J. (1986). Improved Fourier coefficients for maps using phases from partial structures with errors. Acta Crystallogr. *A42*, 140–149.

Renault, L., Nassar, N., Vetter, I., Becker, J., Klebe, C., Roth, M., and Wittinghofer, A. (1998). The 1.7 Å crystal structure of the regulator of chromosome condensation (RCC1) reveals a seven-bladed propeller. Nature *392*, 97–101.

Ron, D., Zannini, M., Lewis, M., Wickner, R.B., Hunt, L.T., Graziani, G., Tronick, S.R., Aaronson, S.A., and Eva, A. (1991). A region of proto-*dbl* essential for its transforming activity shows sequence similarity to a yeast cell cycle gene, CDC24, and the human breakpoint cluster gene, *bcr*. The New Biologist *3*, 372–379.

Steven, R., Kubiseski, T.J., Zheng, H., Kulkarni, S., Mancillas, J., Morales, A.R., Hogue, C.W.V., Pawson, T., and Cuolotti, J. (1998). UNC-73 activates the Rac GTPase and is required for cell and growth cone migrations in *C. elegans*. Cell *92*, 785–795.

Wang, Y., Jiang, Y., Meyering-Voss, M., Sprinzl, M., and Sigler, P.B. (1997). Crystal structure of the Ef-Tu/Ef-Ts complex from *Thermus thermophilus*. Nat. Struct. Biol. *4*, 650–656.

Whitehead, I.P., Khoshravi-Far, R., Kirk, H., Trigio-Gonzalez, G., Der, C.J., and Kay, R. (1996). Expression cloning of *lsc*, a novel oncogene with structural similarities to the Dbl family of guanine nucleotide exchange factors. J. Biol. Chem. *271*, 18643–18650.

Whitehead, I.P., Campbell, S., Rossman, K.L., and Der, C.J. (1997). Dbl family proteins. Biochem. Biophys. Acta *1332*, F1-F23.

Yao, L., Kawakami, Y., and Kawakami, T. (1994). The pleckstrin homology domain of Bruton tyrosine kinase interacts with protein kinase C. Proc. Natl. Acad. Sci. USA *91*, 9175–9179.

Yu, H., and Schreiber, S.L. (1995). Structure of guanine nucleotide-exchange factor human Mss4 and identification of its Rab-interacting surface. Nature *376*, 788–791.

Zheng, Y., Cerione, R., and Bender, A. (1994). Control of the yeast bud-site assembly GTPase Cdc42. J. Biol. Chem. *269*, 2369–2372.

Zheng, Y., Olson, M.F., Hall, A., Cerione, R.A., and Toksoz, D. (1995). Direct-involvement of the small GTP-binding protein Rho in *lbc* oncogene function. J. Biol. Chem. *270*, 9031–9034.

Zheng, J., Chen, R.-H., Corblan-Garcia, S., Cahill, S.M., Bar-Sagi, D., and Cowburn, D. (1997). The solution structure of the pleckstrin homology domain of human Sos1. J. Biol. Chem. *272*, 30340–30344.